arXiv:1608.08661v1 [hep-ex] 30 Aug 2016

Z-dark search with the ATLAS detector

Elizabeth Castaneda-Miranda
Department of Physics, University of Johannesburg, South Africa
E-mail: elizabeth.castaneda.miranda@cern.ch

Abstract. The search of the "hidden sector" via new neutral light bosons Z-dark (Z_d) could be revealed by the study of the decay of the discovered Higgs-like boson or any other undiscovered Higgs boson. After the LHC concluded a successful first period of running, the ATLAS Collaboration published its latest results on the $H \to Z_d Z_d \to 4l$ analysis using up to 20 fb^{-1} of integrated luminosity at $\sqrt{s} = 8$ TeV. In this proceeding I present a summary of the recent results on the search of the Z_d in the signature $H \to Z_d Z_d \to 4l$ with the ATLAS detector at the LHC.

1. Introduction

The $H \to Z_d Z_d \to 4l$ is an interesting search compatible with one of the main decay channels used in the discovery of the SM Higgs boson, $H \to ZZ^* \to 4l$ [1]. This search is motivated by many extensions to the Standard Model (SM) which provide a candidate for the dark force mediator to explain the astrophysical observations of the positron excess [2], or a candidate mediator of the "hidden or dark sector" [3, 4, 5].

This document presents the results on the Z_d search, for both model independent and dependent cases. The study is based on the SM $H \to ZZ^* \to 4l$ [1, 6], with objective to find a significant excess in the dilepton mass region $15 \leq m_{Z_d \to ll} \leq 60$ GeV, with a Higgs mass fixed $m_H = 125$ GeV. Otherwise, 95% upper bound are set on the main parameters of interest as a function of the m_{Z_d}. The information presented here is reported and published by the ATLAS Collaboration [7].

2. The ATLAS detector

It is a multipurpose detector located at point 1 at the LHC. Generally speaking, the ATLAS detector consists of four major subsystems: Inner Detector (ID), Calorimeter, Muon Spectrometer (MS) and Magnet System. These subsystems are integrated with the following components: Trigger and Data Acquisition System and Computing System [8, 9]. The coordinate system used in ATLAS is the right-handed with origin at interaction point in the center of the detector, the z-axis along the beam line and the x-y plane perpendicular to the beam line. Cylindrical coordinates (r, ϕ) are used in the transverse plane, ϕ is the azimuthal angle around the beam line. Observables labelled "transverse" are projected into the x-y plane. The pseudorapidity is defined in terms of the polar angle θ as $\eta = -\ln \tan \theta/2$.

3. Signal and background simulation samples

The new neutral light boson is produced via the Higgs boson production ($H \to Z_d Z_d \to 4l$) in the gluon fusion (ggF). The benchmark model used is the hidden Abelian Higgs model

Table 1. List of the background processes and their corresponding event generators, PDF's calculators, and their QCD and EW applied corrections. The references of the generators, used for this study, are found in [7].

Process	Generator	PDF	QCD corr.	EW corr.
ggFF, VBF	POWHEG+PYTHIA8	CT10	NLO and NNLO	NLO
WH, ZH	PYTHIA8	CT10	NNLO	NLO
$t\bar{t}$H	PYTHIA8	CTEQ6L1	NLO	—
$q\bar{q} \to$ ZZ*	POWHEG+PYTHIA8	CT10	NLO	—
gg $\to$ ZZ*	gg2ZZ+JIMMY	CT10	NLO	—
Z+jets	ALPGEN	CTEQ6L1	NLO and NNLO	—
$t\bar{t}$	MC@NLO+HERWIG, JIMMY	CT10	NLO	—
WZ and WW	SHERPA	CT10	NLO	—
ZJ/ψ, ZΥ	PYTHIA8	CTEQ6L1	—	—

(HAHM) [3, 4, 5]. The samples are generated for $m_H = 125$ GeV and $15 \leq m_{Z_d} \leq 60$ GeV, in steps of 5 GeV, using MadGraph with CTEQ6L1 for the parton distribution functions (PDF). For taking into account the parton showering, hadronization, and initial- and final-state radiation PYTHIA8 and PHOTOS are used. In the $H \to Z_d Z_d \to 4l$ search, the $h \to 4l$ is normalized from data.

The background processes considered for this study are listed in Table 1. For the SM Higgs boson in ggF production, the QCD soft-gluon resummations, calculated in the next-to-next-to-leading-logarithmic (NNLL) approximation, are applied. The Z+jets production, modelled with up to five partons, is divided in two sources: Z+light-jets and $Zb\bar{b}$. For data and simulation comparison, the QCD cross-section calculations (see Table 1) are used to normalize the simulation for inclusive Z boson and $Zb\bar{b}$ production. The ZJ/ψ and $Z\Upsilon$ Monte Carlo (MC) samples are normalized using the ATLAS measurement described in [10]. The SM Higgs productions, SM ZZ^* and diboson processes are normalized with the theoretical cross-sections and decay branching ratios as well as their uncertainties. For taking into account the different conditions in the pileup, as a function of the instantaneous luminosity, the simulated minimun-bias overlayed events, generated with PYTHIA8 onto the hard-scattering process, were used. Such events were reweighted according to the distribution of the mean number of interactions observed in data. All the MC background samples generated are reconstructed using the "full detector simulation" ATLAS software [11] which is based on GEANT4 [12]. The signal samples are reconstructed with the "fast detector simulation" ATLAS software [13] which only parametrized the response of the electromagnetic and hadronic showers in the ATLAS calorimeter, and the rest of the systems are reconstructed as "full detector simulation".

4. Event selection

For this search, 20.3 fb^{-1} of integrated luminosity is used which was recorded in the optimal function of the detector. All the MC processes are normalized with integrated luminosity mentioned. The event selection applied is the same for both data and MC. There are three categories that are studied: 4−electrons ($4e$), 4−muons (4μ) and 2−electrons 2−muons ($2e2\mu$).

It is requested that the (data/MC) events pass the combination of single-lepton and dilepton triggers. Table 2 shows the list of single-lepton and dilepton triggers used, with their respective thresholds in transverse energy/momentum. All these events must contain a reconstructed primary vertex, defined as the vertex with highest $\sum p_T^2$ of the associated tracks, with at least three tracks of $p_T > 0.4$ GeV each one. The muon candidates selected are formed by matching reconstructed ID tracks with either a complete track or track-segment reconstructed in MS

Table 2. Triggers used with their respective E_T or p_T thresholds.

Trigger	E_T [GeV]	p_T [GeV]
single-electron	25	—
single-muon	—	24
dielectron	12	—
dimuon (symm.)	—	13
dimuon (asymm.)	—	18 and 8
electron-muon	12 or 24	8

[14]. The acceptance is extended using tracks reconstructed in the forward region of the MS ($2.5 < |\eta| < 2.7$), which is outside the ID coverage. If both an ID or a complete MS track are present, the two independent momentum measurements are combined; otherwise the information of the ID or the MS is used alone. In the case of the electrons candidates, they must have well-reconstructed ID track pointing to an electromagnetic calorimeter cluster and the cluster should satisfy a set of identification criteria [15]. Tracks associated with electromagnetic clusters are fitted using a Gaussian-Sum Filter [15], which allows for bremsstrahlung energy losses to be taken into account. Each electron (muon) must satisfy $p_T > 7$ GeV ($p_T > 6$ GeV) and be measured in the range $|\eta| < 2.47$ ($|\eta| < 2.7$). The longitudinal impact parameters of the leptons along the beam axis z_0 are required to be within 10 mm of the reconstructed primary vertex (muons without ID track are exempted of this requirement). To reject the cosmic rays, muon tracks are required to have a transverse impact parameter d_0 (closest approach to the primary vertex in the x-y plane) of less than 1mm. For avoiding double-counting of leptons, an overlap removal is applied. If two electrons share the same ID track or within in a cone ($\Delta R \equiv \sqrt{(\Delta\phi)^2 + (\Delta\eta)^2} < 0.1$), the one with the highest transverse energy deposit in the calorimeter (E_T) is kept. An electron within in a muon cone ($\Delta R = 0.2$) is removed, and a calorimeter-based reconstructed muon within an electron cone ($\Delta R = 0.2$) is removed.

After selecting the leptons with proper quality, events with at least four leptons, with all possible combinations of four leptons containing two same-flavor and opposite-sign (SFOS) defined the "quadruplets", are kept. Each lepton is ordered by p_T, the three highest-p_T leptons should have: $p_{Tl1} > 20$ GeV, $p_{Tl2} > 15$ GeV and $p_{Tl3} > 10$ GeV. It is also required that at least one (two) of the lepton(s), from the quadruplet, must satisfy the single-lepton (dilepton) trigger requirements. Each dilepton invariant mass or each SFOS pair, from the quadruplet, are denoted by m_{12} (formed by leptons 1 and 2) and m_{34} (formed by leptons 3 and 4). For the $H \to Z_d Z_d \to 4l$ study, both Z_d boson are considered to be on-shell, because of that, there is not any distinction between the SFOS pairs. If in the event there are several "quadruplets", only the quadruplet that satisfies the minimum value of $\Delta m \equiv |m_{12} - m_{34}|$ is selected. Subsequently, the transverse impact parameter significance (IP) and the isolation requirements are imposed to the leptons of the quadruplet selected, and four final requirements that defined the two signal regions (SR) considered in this study are shown in Table 3. In Figs. 1 and 2 show the dilepton and four-lepton invariant masses after the IP requirements, respectively, in the dilepton mass the m_{12} and m_{34} are combined.

5. Background estimation

For the $H \to Z_d Z_d \to 4l$ analysis, the main background contributions are $ZZ^* \to 4l$ and $H \to ZZ^* \to 4l$ which are reduced considerably after applying the tight SR (see Table 3). Also small contribution from Z+jets, $t\bar{t}$, WW and WZ can be seen from Fig. 3. The $H \to ZZ^* \to 4l$, $ZZ^* \to 4l$, WW and WZ background processes are estimated from MC

Table 3. Requirements after selecting the one quadruplet, and the loose and tight SR definitions.

Requirements	
Track isolation	$\frac{\sum p_T^{tracks}}{p_T^{lepton}}(\Delta R = 0.2) < 0.15$
Calorimeter isolation	$\frac{\sum E_T^{clusters}}{E_T^e(p_T^\mu)}(\Delta R = 0.2)$ <0.2 (0.3 and μ's no ID 0.15)
IP	$\frac{d_0}{\sigma_0^{IP\ uncer.}} < 6.5$ for e's (3.5 for μ's)
Loose SR	$115 < m_4 < 130$ GeV, $\lvert m_{Z_d} - m_{ll}\rvert < \frac{m_H}{2}$, $m_H = 125$ GeV, and Z, $J/\psi - \Upsilon$ vetoes: $\lvert m_{Z_{PDG}} - m_{ll}\rvert < 10$ GeV, $m_{ll} < 12$ GeV (ll=12,34, and 23, 14)
Tight SR	Loose SR and $\lvert m_{Z_d} - m_{ll}\rvert < \delta m$ (5/3/4.5 GeV for $4e/4\mu/2e2\mu$)

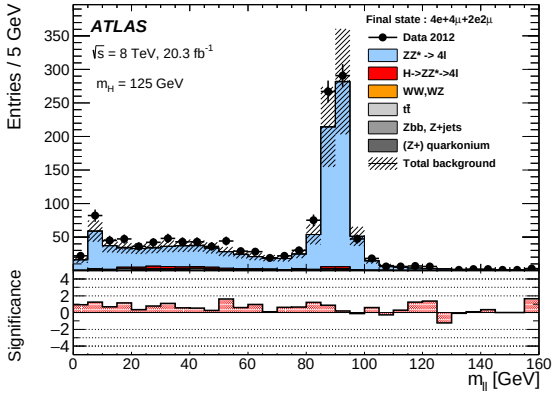

Figure 1. Dilepton invariant mass $m_{ll=12,34}$ for $m_H = 125$ GeV at the IP requirements.

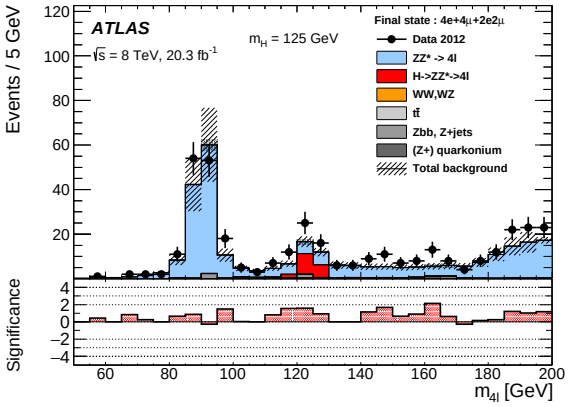

Figure 2. Four-lepton invariant mass for $m_H = 125$ GeV at the IP requirements.

simulation, their normalization is based on theoretical cross-sections calculations, integrated luminosity recorded, and acceptance efficiency. In the case of zero MC background expected events, in the tight SR, 68% C.L. upper bound, which corresponds to 1.14 events [16], is estimated as $N_{background} < L \times \sigma \times \frac{1.14}{N_{total}}$, where L is the integrated luminosity recorded, σ the cross-section of the background processes and N_{tot} is the total number of weighted events simulated for the background processes. This background estimation is validated using a control region defined by reversing, the four-lepton invariant mass requirement ($m_{4l} < 115$ GeV or $m_{4l} > 115$ GeV), good agreement is found between the expectation and observation results [7].

6. Systematic uncertainties

The systematic uncertainties on the theoretical cross-section calculations as well as the detector uncertainties are taken into account. The PDF effects, α_s, renormalization and factorization scale uncertainties are applied to the ZZ^* backgrounds, and for all the SM Higgs productions applied on the total inclusive cross-sections, using values obtained from [17]. Uncertainties due to the limited number of MC events in the $t\bar{t}$, Z+jets, ZJ/ψ, $Z\Upsilon$ and WW/WZ background processes are estimated (see Sec. 5). The luminosity uncertainty [18] is applied to all signal and background yields. The detector systematic uncertainties on the electron and muons, within the acceptance on SR, are applied (see Table 4): uncertainties on electron/muon identification,

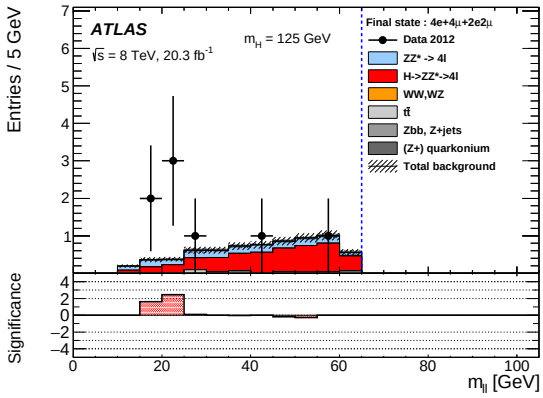

Figure 3. Dilepton invariant mass $m_{ll=12,34}$ for $m_H = 125$ GeV at the Loose SR.

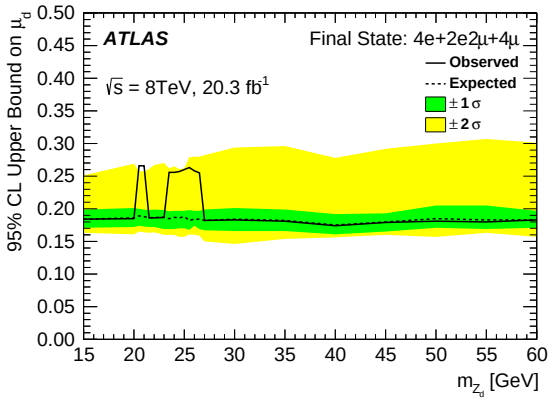

Figure 4. The 95% C.L. upper bound on the signal strength μ_d, see Eq 1.

Table 4. Relative systematic uncertainties on the event yields.

Source	4μ	$4e$	$2e2\mu$
Electron identification	—	6.7	3.2
Electron energy scale	—	0.8	0.3
Muon identification	2.6	—	1.3
Muon momentum scale	0.1	—	0.1
Luminosity	2.8	2.8	2.8
ggF QCD	7.8	7.8	7.8
ggF PDF's and α_s	7.5	7.5	7.5
ZZ* Normalization	5.0	5.0	5.0

reconstruction and trigger efficiency (summarized in Electron/Muon identification), on the electron/muon energy/momentum scale, and on the electron/muon energy/momentum resolution (summarized in Electron/Muon energy/momentum scale). Also the uncertainties from the isolation and IP requirements are taken into account.

7. Results

Four data events pass after applying the loose SR requirements: one in the $4e$, two in the 4μ and one in the $2e2\mu$ channel. Only two of these events pass the tight SR: the event in the $4e$ and one of the events in the 4μ channel. The events in $4e$ and 4μ channels are consistent with the Z_d mass range $23.5 \leq m_{Z_d} \leq 26.5$ GeV and $20.5 \leq m_{Z_d} \leq 21.0$ GeV, respectively, as shown in Fig. 3. In the mass range of 15 to 60 GeV the interpolated histograms are used [19], generated, based on the MC signal simulations, in steps of 0.5 GeV to obtain the signal acceptance at the hypothesized m_{Z_d}. Table 5 shows the expected and observed number of events after applying the tight SR requirements. In the absence of any significant excess, the 95% C.L. upper bound is computed on the parameter of interest, the signal strength, which is defined as:

$$\mu_d = \frac{\sigma \times BR(H \to Z_d Z_d \to 4l)}{[\sigma \times BR(H \to ZZ^* \to 4l)]_{SM}}. \quad (1)$$

The limits are computed for each final state and their combination for the model independent case, following the CL_s modified frequentist formalism with the profile-likelihood test

Table 5. The expected and observed number of events in the tight signal region for each final state are shown. The results are for the mass regions $m_{Z_d} = 25$ and 20.5 GeV. The statistical and systematic uncertainties are given for the signal and background expected events. The $H \to ZZ^* \to 4l$ expected events are the combination of the ggF, VBF, ZH, WH and $t\bar{t}H$ processes.

Process	$4e$	4μ	$2e2\mu$
$H \to ZZ^* \to 4l$	$(1.5 \pm 0.3 \pm 0.2) \times 10^{-2}$	$(1.0 \pm 0.3 \pm 0.3) \times 10^{-2}$	$(2.9 \pm 1.0 \pm 2.0) \times 10^{-3}$
$ZZ^* \to 4l$	$(7.1 \pm 3.6 \pm 0.5) \times 10^{-4}$	$(8.4 \pm 3.8 \pm 0.5) \times 10^{-3}$	$(9.1 \pm 3.6 \pm 0.6) \times 10^{-3}$
WW, WZ	$< 0.7 \times 10^{-2}$	$< 0.7 \times 10^{-2}$	$< 0.7 \times 10^{-2}$
$t\bar{t}$	$< 3.0 \times 10^{-2}$	$< 3.0 \times 10^{-2}$	$< 3.0 \times 10^{-2}$
Zbb, Z+jets	$< 0.2 \times 10^{-2}$	$< 0.2 \times 10^{-2}$	$< 0.2 \times 10^{-2}$
ZJ/ψ, $Z\Upsilon$	$< 2.3 \times 10^{-3}$	$< 2.3 \times 10^{-3}$	$< 2.3 \times 10^{-3}$
Total background	$< 5.6 \times 10^{-2}$	$< 5.9 \times 10^{-2}$	$< 5.3 \times 10^{-2}$
Data	1	0	0
$H \to ZZ^* \to 4l$	$(1.2 \pm 0.3 \pm 0.2) \times 10^{-2}$	$(5.8 \pm 2.0 \pm 2.0) \times 10^{-3}$	$(2.6 \pm 1.0 \pm 0.2) \times 10^{-3}$
$ZZ^* \to 4l$	$(3.5 \pm 2.0 \pm 0.2) \times 10^{-3}$	$(4.1 \pm 2.7 \pm 0.2) \times 10^{-3}$	$(2.0 \pm 0.6 \pm 0.1) \times 10^{-2}$
WW, WZ	$< 0.7 \times 10^{-2}$	$< 0.7 \times 10^{-2}$	$< 0.7 \times 10^{-2}$
$t\bar{t}$	$< 3.0 \times 10^{-2}$	$< 3.0 \times 10^{-2}$	$< 3.0 \times 10^{-2}$
Zbb, Z+jets	$< 0.2 \times 10^{-2}$	$< 0.2 \times 10^{-2}$	$< 0.2 \times 10^{-2}$
ZJ/ψ, $Z\Upsilon$	$< 2.3 \times 10^{-3}$	$< 2.3 \times 10^{-3}$	$< 2.3 \times 10^{-3}$
Total background	$< 5.3 \times 10^{-2}$	$< 5.1 \times 10^{-2}$	$< 6.4 \times 10^{-2}$
Data	0	1	0

statistic [20]. The nuisance parameters associated with the systematic uncertainties described in Sec 6 are profiled. The systematic uncertainties on Table 4 are 100% correlated between the signal and background. In Figs. 4 and 5 show the 95% C.L. upper bound on the μ_d and on the branching ratio of $H \to Z_d Z_d \to 4l$ as a function of the mass m_{Z_d} for the combination of the three final states: $4e$, 4μ and $2e2\mu$; assuming the SM Higgs boson cross-section and $BR(H \to ZZ^* \to 4l)_{SM} = 1.25^{-4}$ [17].

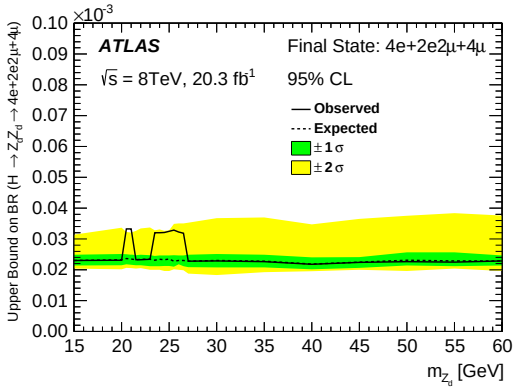

Figure 5. The 95% C.L. upper bound on the $BR(H \to Z_d Z_d \to 4l)$.

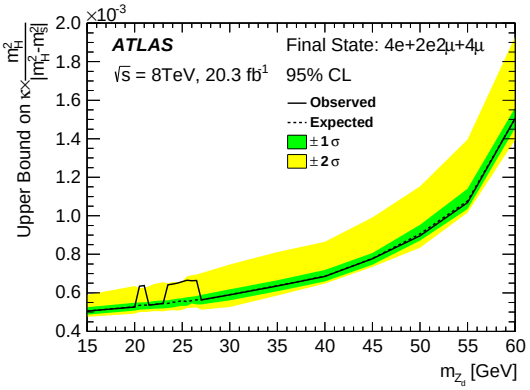

Figure 6. The 95% C.L. upper bound on the Higgs mixing parameter, see Eq. 2.

For the model dependent case, the simplest benchmark model is the SM plus a dark vector boson and a dark Higgs boson [3, 4, 5], where the branching ratio of the $Z_d \to ll$ is given as a function of the m_{Z_d}, which can be used to convert the upper bound measurement of the μ_d into an upper bound on the branching ratio BR($H \to Z_d Z_d$), assuming the SM Higgs production

cross-section [7]. The $H \to Z_d Z_d$ decay can be used to obtain an $m_{Z_d}-$dependent limit on an Higgs mixing parameter κ' [4]:

$$\kappa' = \kappa \times \frac{m_H^2}{|m_H^2 - m_s^2|}, \tag{2}$$

where κ is the size of the Higgs portal coupling and m_s is the mass of the dark Higgs boson. The partial width of the $H \to Z_d Z_d$ is given in terms of κ [4]. In the regime where the Higgs mixing parameter dominates ($\kappa \gg \epsilon$), $m_s > m_H/2$, $m_{Z_d} < m_H/2$ and $H \to Z_d Z^* \to 4l$ are negligible, the only relevant decay is $H \to Z_d Z_d$. The Higgs portal coupling parameter κ is [4]:

$$\kappa^2 = \frac{\Gamma_{SM}}{f(m_{Z_d})} \frac{BR(H \to Z_d Z_d)}{1 - BR(H \to Z_d Z_d)}. \tag{3}$$

The upper bound on the effective Higgs mixing parameter as a function of m_{Z_d} is shown in Fig. 6 for $m_H/2 < m_s < 2m_H$, this corresponds to an upper bound on the Higgs portal coupling in the range $\kappa \sim (1 - 10) \times 10^{-4}$.

8. Conclusions

The search of the Z_d light boson in a mass range of $15 \leq m_{Z_d} \leq 60$ GeV, via $H \to Z_d Z_d \to 4l$ with $m_H = 125$ GeV, is presented at $\sqrt{s} = 8$ TeV. Two data events in the tight SR are observed in $4e$ and 4μ final states: $4e$, $m_{Z_{d1,2}} = 21.8,\ 28.1$ GeV and 4μ, $m_{Z_{d1,2}} = 23.2,\ 18.0$ GeV. Since there is not significant excess observed, the 95% C.L. upper bound on the μ_d, and on the $BR(H \to Z_d Z_d \to 4l)$ are set, combining the three final states. For the mass range $20 \leq m_{Z_d} \leq 28$ GeV, in the model independent case, the upper bounds for μ_d are $(18-27)\times 10^{-2}$; in case of the model depending study, the upper bound for the $BR(H \to Z_d Z_d \to 4l)$ is $(2.1 - 3.2) \times 10^{-5}$, and the upper bound on the Higgs mixing parameter is $(5.0 - 6.5) \times 10^{-4}$ (see Fig. 4, 5 and 6).

8.1. Acknowledgments

It is a pleasure to thank the ATLAS Collaboration, to CONACyT for the support received as a postdoctoral fellow with the University of Johannesburg, to Professor Simon Connell, Ketevi Assamagan and the University of Cape Town for giving me the opportunity to be part of the SouthAfrican group in the ATLAS Collaboration and for working in this project.

References

[1] The ATLAS Collaboration 2012 *Phys. Lett.* B **716** 1
[2] The AMS Collaboration 2013 *Phys. Rev. Lett.* **110** 141102
[3] S. Gopalakrishna, S. Jung, and J. D. Wells 2008 *Phys. Rev.* D **78** 055002; J. D. Wells 2008 *arXiv:0803.1243*
[4] D. Curtin, R Essig, S. Gori, and J. Shelton 2015 *J. High Energy Phys.* **02** 157
[5] D. Curtin *et al.* 2014 *Phys. Rev.* D **90** 075004
[6] The ATLAS Collaboration 2015 *Phys. Rev.* D **91** 012006
[7] The ATLAS Collaboration 2015 *Phys. Rev.* D **92** 092001
[8] The ATLAS Collaboration 2008 *arXiv:0901.0512*
[9] The ATLAS Collaboration 2012 *Eur. Phys. J.* C **72** 1849
[10] The ATLAS Collaboration 2015 *Eur. Phys. J.* C **75** 229
[11] The ATLAS Collaboration 2010 *Eur. Phys. J.* C **70** 823
[12] S. Agostinelli *et al.* 2003 *Nucl. Instrum. Methods Phys. Res.* Sect A **506** 250
[13] The ATLAS Collaboration 2010 *ATL-PHYS-PUB-2010-013*
[14] The ATLAS Collaboration 2011 *ATLAS-CONF-2011-063*
[15] The ATLAS Collaboration 2012 *Eur. Phys. J.* C **72** 1909; *ATLAS-CONF-2012-047*
[16] K. Olive *et al.* 2014 *Chin. Phys.* C **38** 090001
[17] LHC Higgs cross section working group *et al. arXiv: 1101.0593; arXiv:1201.3084*
[18] The ATLAS Collaboration 2013 *Eur. Phys. J.* C **73** 2518
[19] A. L. Read 1999 *Nucl. Instrum. Methods Phys. Res.* Sec. A **425** 357
[20] A. L. Read 2002 *J. Phys.* G **28** 2693; G. Cowan *et al.* 2011 *Eur. Phys. J.* C **71** 1554